Influence of acoustic phonon confinement on electron mobility in ultrathin silicon on insulator layers

L. Donetti, F. Gámiz,[a] N. Rodriguez, F. Jimenez, and C. Sampedro
Departamento de Electrónica y Tecnología de Computadores, Universidad de Granada, 18071 Granada, Spain

(Received 6 November 2005; accepted 21 February 2006; published online 20 March 2006)

We show the importance of acoustic phonon confinement in ultrathin silicon-on-insulator inversion layers by comparing electron mobility calculated by the Monte Carlo method assuming a bulk acoustic phonon model (the usual procedure) with that obtained by using a confined acoustic phonon model developed in this work. Both freestanding and rigid boundary conditions are taken into account for the evaluation of the confined phonon dispersion in a three-layer structure. Mobility reductions of 30% are observed for silicon thicknesses of around 5–10 nm when the confined acoustic phonon model is used. © *2006 American Institute of Physics*. [DOI: 10.1063/1.2187952]

It is widely accepted that progress in silicon device technology will be achieved through the increasing use of very thin silicon-on-insulator (SOI) structures, since SOI devices will become the appropriate vehicle for increasing the operational speed of integrated circuits.[1] However, a recent experimental work,[2] has reported serious mobility degradation in Si ultrathin body (UTB) Metal-oxide-semiconductor field-effect transistors (MOSFETs) with silicon thickness, d_{Si}, smaller than 5 nm. This may suggest serious limitations in achieving SOI goals. The electron transport in ultrathin silicon layers shows substantial modifications when compared to that in bulk silicon inversion layers. Basically, there are three principal phenomena that modify the process of electron scattering in very thin silicon layers. First, reduction of the electron momentum dimensionality and the momentum and energy conservation laws produce a drastic increase in the phonon scattering rate as the silicon thickness decreases;[3] second, the redistribution of the carriers among the different subbands due to quantum effects produces a decrease in the conduction effective mass, and therefore a mobility increase.[3] The third phenomenon arises due to modifications of the phonon modes caused by the acoustic and dielectric mismatches between the silicon and the silicon dioxide. These changes in properties give rise to confined and interface phonons in quantum wells, quantum wires, and quantum dots.[4] The effect of the increase in the phonon scattering rate and the decrease in the conduction effective mass in ultrathin SOI inversion layers have already been studied elsewhere.[3,5] It was shown that electron mobility behavior in SOI devices is a complex function of the silicon thickness as a direct consequence of the superposition of the two opposite effects. With regard to the third phenomenon, confined acoustic phonons have recently been observed in experiments with very thin silicon layers.[4] Over the last few years, some theoretical work has also been developed in III-V based devices.[6,7] There are two main factors that originate from the electron-acoustic phonon scattering, namely, thermal conduction[8] and charge carrier mobility.[7] For this reason, modifications in the phonon spectrum are of strategic interest to device engineers and scientists. Up to now, this phonon confinement has been neglected in the calculation of electron mobility in ultrathin silicon inversion layers, and bulk phonon scattering models have been adopted.[3,9] In this work we provide proof of the importance of acoustic phonon confinement on electron mobility, by calculating electron mobility curves in double gate silicon on insulator (DGSOI) devices for different values of d_{Si} taking into account phonon confinement, and comparing the results to those obtained when phonon confinement is ignored.

In order to physically demonstrate the effect of phonon confinement on very thin silicon layers sandwiched between two oxide layers, we have studied the acoustic phonon quantization in the three-layer structure shown in Fig. 1. The starting point is the elastic continuum model of acoustic phonons (see, for example, Ref. 6): in this model, phonons are represented by elastic waves in a continuous medium. The equation for the displacement vector $\mathbf{u}$ in an isotropic medium can be written as

$$\frac{\partial^2 \mathbf{u}}{\partial t^2} = s_t^2 \nabla^2 \mathbf{u} + (s_l^2 - s_t^2)\, \nabla\, (\nabla \mathbf{u}), \tag{1}$$

where s_t and s_l are the transversal and longitudinal sound speeds, respectively.

We have solved the above equation assuming the structure shown in Fig. 1 with different boundary conditions. For simplicity, to maintain the symmetry of the system, we consider two layers of silicon dioxide of equal thickness d_{ox} around a layer of silicon of thickness d_{Si}. This does not imply any loss of generality since the model can also be applied to structures with unequal top and bottom oxide thicknesses. We look for normalized solutions in the form:

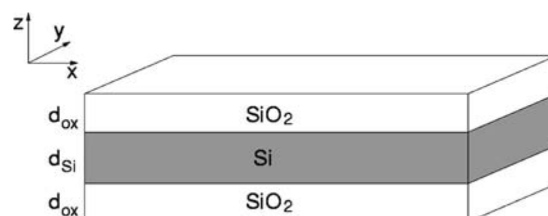

FIG. 1. Device structure considered for the study of phonon quantization.

[a]Electronic mail: fgamiz@ugr.es

 © 2006 American Institute of Physics

$$\mathbf{u}(\mathbf{r}_\parallel,z)=\mathbf{w}_n(\mathbf{q}_\parallel,z)e^{i\mathbf{q}_\parallel\cdot\mathbf{r}_\parallel-i\omega_n t}, \quad (2)$$

where $\parallel$ denotes vector components in the xy plane, which is the plane parallel to the Si-SiO_2 interfaces.

The usual quantization rules then yield the representation of the displacement $\mathbf{u}$ in terms of phonons:

$$\mathbf{u}=\sum_{\mathbf{q}_\parallel,n}\sqrt{\frac{\hbar}{2A\rho\omega_n}}[a_n(\mathbf{q}_\parallel)+a_n^\dagger(-\mathbf{q}_\parallel)]\mathbf{w}_n(\mathbf{q}_\parallel,z)\mathrm{e}^{i\mathbf{q}_\parallel\cdot\mathbf{r}_\parallel-i\omega_n t}, \quad (3)$$

where a_n and $a_n^\dagger$ are the creation and annihilation operators of phonons, A denotes the area of the layer in the xy plane, and ρ the material density. The interaction Hamiltonian then reads

$$H_{\mathrm{int}}=D_{\mathrm{ac}}\nabla\mathbf{u}=D_{\mathrm{ac}}\sum_{\mathbf{q}_\parallel,n}\sqrt{\frac{\hbar}{2A\rho\omega_n}}[a_n(\mathbf{q}_\parallel)+a_n^\dagger(-\mathbf{q}_\parallel)]\Gamma(z)e^{i\mathbf{q}_\parallel\cdot\mathbf{r}_\parallel-i\omega_n t}, \quad (4)$$

where

$$\Gamma(z)=i\mathbf{q}_\parallel\cdot\mathbf{w}_n(\mathbf{q}_\parallel,z)+\frac{\partial w_{n,z}(\mathbf{q}_\parallel,z)}{\partial z} \quad (5)$$

and D_{ac} is the acoustic phonon deformation potential parameter.

Without loss of generality we can assume that $\mathbf{q}_\parallel$ is directed along the x axis, that is, $\mathbf{q}_\parallel=(q,0)$; the equations for the components of $\mathbf{w}$ follow:

$$-\omega^2 w_x(z)=\left(s_t^2\frac{d^2}{dz^2}-s_l^2q^2\right)w_x(z)+i(s_l^2-s_t^2)q\frac{d}{dz}w_z(z),$$

$$-\omega^2 w_y(z)=s_t^2\left(\frac{d^2}{dz^2}-q^2\right)w_y(z), \quad (6)$$

$$-\omega^2 w_z(z)=\left(s_l^2\frac{d^2}{dz^2}-s_t^2q^2\right)w_z(z)+i(s_l^2-s_t^2)q\frac{d}{dz}w_x(z).$$

The y component is decoupled from the others, giving solutions where the only nonzero component is w_y; these are known as shear waves. Shear waves have a vanishing interaction Hamiltonian, according to Eqs. (4) and (5).

The x and z components however, are coupled and, due to the symmetry of the system around the middle of the structure, we can classify the solutions as those with symmetric x and antisymmetric z components (SA waves) and those with antisymmetric x and symmetric z components (AS waves). In the silicon layer, the SA waves consist of a linear combination of a symmetric w_x and an antisymmetric w_z (known as dilatational waves) while the AS waves consist of a linear combination of an antisymmetric w_x and a symmetric w_z (known as flexural waves). In both cases, SA and AS waves, the solution in the two oxide layers is a linear combination of all four solutions; the actual solution must fulfill continuity equations for w_x, w_z, T_{xz}, T_{zz} at the interface between silicon and oxide, and must be subject to the boundary conditions at the external surfaces [i.e., $z=\pm(d_{\mathrm{Si}}/2+d_{\mathrm{ox}})$], T_{xz}, T_{zz} being components of the stress tensor given by

$$T_{xz}=\rho s_t^2\left(\frac{dw_x}{dz}+iqw_z\right), \quad (7)$$

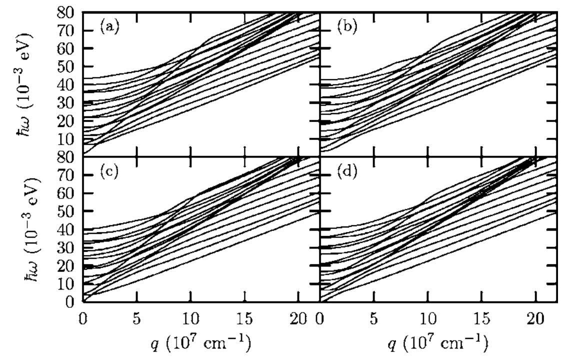

FIG. 2. Some branches of the dispersion relation for a structure with $d_{\mathrm{Si}}=2$ nm and $d_{\mathrm{ox}}=1$ nm; (a) and (b) are the SA and AS waves for the rigid surface boundary conditions; and (c) and (d) the same for free boundary conditions.

$$T_{zz}=\rho\left(s_l^2\frac{dw_z}{dz}+iq(s_l^2-2s_t^2)w_x\right). \quad (8)$$

We have considered two types of boundary conditions: (i) rigid boundary conditions (RBC) and (ii) freestanding boundary conditions (FBC). In the former case, RBC, the displacement vector must vanish on the external surfaces, i.e., $u=0$.[10] In the latter case, FBC, the z components of the stress tensor, (T_{xz}, T_{yz}, T_{zz}) must vanish[6,11] on the external surfaces. In both cases, we obtain a system of six linear homogenous equations with six unknowns (the coefficients of the two components in the silicon layer and the four in the oxide layers). Figure 2 shows corresponding dispersion branches (15 AS + 15 SA branches) for the structure shown in Fig. 1, assuming $d_{\mathrm{Si}}=2$ nm, and $d_{\mathrm{ox}}=1$ nm.

Once the dispersion relations have been computed for the phonons in thin layers, we can evaluate the interaction Hamiltonian taking into account Eqs. (4) and (5) and then calculate the scattering rates. The starting point for the calculation of the scattering rate is the *Fermi golden rule*, which gives the transition probability density between two states i and f:

$$W_{i\to f}=\frac{2\pi}{\hbar}|\langle f|H_{\mathrm{int}}|i\rangle|^2\delta(\epsilon_f-\epsilon_i), \quad (9)$$

where the initial and the final states contain both the electron and the phonon states. The scattering rate is then obtained by integrating over the final state of the electron, and taking into account the contributions of phonon absorption or emission, of different phonon types (AS or SA) and phonon dispersion branches.[11] Figure 3 shows the ratio of the scattering rate with that obtained using a bulk model with elastic approximation, as a function of the initial electron energy, for different layer thicknesses. Note that only the intrasubband scattering rate for an electron in the first subband is shown in the graph. For both sets of boundary conditions, the phonon scattering rates for the confined model are higher than the corresponding ones for bulk models, and significantly increase as the silicon thickness decreases.

We used this confined acoustic phonon model in a Monte Carlo simulator to evaluate the electron mobility as a function of the silicon thickness in a double gate SOI MOSFET. A description of the Monte Carlo simulator used can be found elsewhere.[3] Only phonon scattering was taken into account. Intervalley optical phonons were taken into account assuming the usual bulk model [for a recent analysis of in-

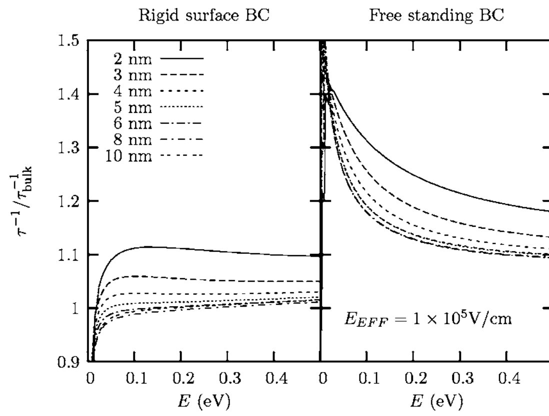

FIG. 3. Confined acoustic phonon scattering rate normalized to the bulk elastic scattering rate, as a function of initial electron energy, for different silicon layer thicknesses in a DGSOI device. The oxide thickness used for this calculation is 1 nm.

tervalley phonon scattering beyond the bulk model see [Ref. 12]. We can observe in Fig. 4 that a significant reduction in electron mobility occurs when the confined phonon model is considered, regardless of the boundary condition set, the effect being greater for freestanding boundary conditions. The most important corrections (which could reach almost 30%)

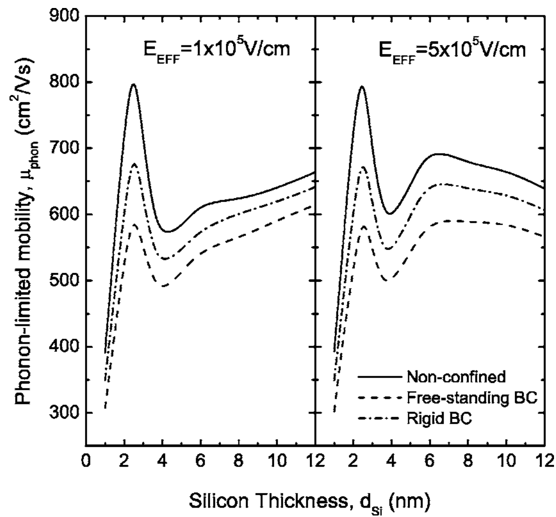

FIG. 4. Calculated electron mobility in double gate silicon-on-insulator inversion layers vs the silicon thickness for two values of the transverse effective field. The oxide thickness was taken as 1 nm. Solid line: bulk acoustic phonon model; dashed line: confined acoustic phonon with freestanding boundary conditions; dash-dotted line: confined acoustic phonon with rigid boundary conditions.

correspond to silicon thicknesses in the range of 5–10 nm where previous results obtained with a bulk acoustic phonon model showed a considerable mobility increase due to the volume inversion effect.[3] Our results mean that the goodness of volume inversion effect on electron mobility, although still present, is certainly modulated by the phonon scattering confinement which has been systematically ignored in previous works. Clearly, the presence of other scattering mechanisms (notably interface roughness scattering) also limit the electron mobility; the effect of acoustic phonon confinement in this case could be smaller but still important.

In conclusion, we have shown the importance of acoustic phonon confinement in ultrathin SOI inversion layers by comparing electron mobility in ultrathin DGSOI devices, calculated assuming a bulk acoustic phonon model (the usual procedure) and using the confined acoustic phonon model developed in this work. We have shown that mobility reductions of around 30% are obtained when the confined acoustic phonon model is used. It is therefore essential to include such models in the electron transport simulations of ultrathin SOI devices if we want to capture the actual behavior of electrons in silicon layers of nanometric thickness.

This work has been partially carried out within the framework of Research Projects FIS2005-06832 and TEC-2005-01948 supported by the Spanish Government, and by EU (Network of Excellence SINANO, Contract No. IST-1-506844-NoE).

[1]G. C. Celler and S. Cristoloveanu, J. Appl. Phys. **93**, 4955 (2003).
[2]K. Uchida and S. Takagi, Appl. Phys. Lett. **82**, 2916 (2003).
[3]F. Gámiz and M. V. Fischetti, J. Appl. Phys. **89**, 5478 (2001).
[4]C. M. Sotomayor Torres, A. Zwick, F. Poinsotte, J. Groenen, M. Prunilla, J. Ahopelto, A. Mlayah, and V. Paillard, Phys. Status Solidi C **1**, 2609 (2004).
[5]F. Gámiz, J. B. Roldán, P. Cartujo-Cassinello, J. E. Carceller, J. A. López-Villanueva, and S. Rodriguez, J. Appl. Phys. **86**, 6269 (1999).
[6]N. Bannov, V. Mitin, and M. Stroscio, Phys. Status Solidi B **183**, 131 (1994).
[7]E. P. Pokatilova, D. L. Nikaa, and A. A. Balandin, Superlattices Microstruct. **33**, 155- (2003).
[8]M. Asheghi, Y. K. Leung, S. S. Wong, and K. E. Goodson, Appl. Phys. Lett. **71**, 1798- (1997).
[9]P. Palestri, S. Eminente, D. Esseni, C. Fiegna, E. Sangiorgi, and L. Selmi, Solid-State Electron. **49**, 727 (2005).
[10]B. A. Glavin, V. I. Pipa, V. V. Mitin, and M. A. Stroscio, Phys. Rev. B **65**, 205315 (2002).
[11]N. Bannov, V. Aristov, V. Mitin, and M. A. Stroscio, Phys. Rev. B **51**, 9930 (1995).
[12]M. Prunilla, P. Kivinen, A. Savin, P. Törmä, and J. Ahopelto, Phys. Rev. Lett. **95**, 226602 (2005).

Applied Physics Letters is copyrighted by the American Institute of Physics (AIP). Redistribution of journal material is subject to the AIP online journal license and/or AIP copyright. For more information, see http://ojps.aip.org/aplo/aplcr.jsp